Numerical and Experimental Analysis of Heat Transfer and Fluid Flow in 3-D Circular Finned-Tube Heat Exchangers

J. Y. Jang and J. T. Lai

Department of Mechanical Engineering, National Cheng-Kung University, Tainan, Taiwan

ABSTRACT

Fluid flow and heat transfer over a 4 row circular finned- tube heat exchanger are studied numerically and experimentally. Two types of finned-tube configurations have been investigated under the dry and wet conditions for different values of inlet frontal velocity ranging from 2 to 6 m/s. The experimental results indicated that the sensible Colburn factor j_S for the wet coils is 20 % higher than that for the dry coils; the friction factor f for the wet coils is 15 % higher than that for the dry coils. The three-dimensional numerical results of laminar model for the pressure drop are in good agreement with the experimental data, while overestimate 200% of the heat transfer coefficient.

1. INTRODUCTION

The reported thermal-hydraulic performance data of the circular finned-tube heat exchangers were experimental in nature. A substantial amount of performance data on the dry coils has been published, and several heat transfer and pressure drop correlations have been proposed. Webb[1] provides a survey of the published data and correlations. He recommended the Briggs and Young [2] correlation for heat transfer , and the Robinson and Briggs [3] correlation for pressure drop. Both correlations are empirically based and are valid for four or more tube rows. Idem et al. [4-5] reported the convective heat & mass transfer coefficients and friction factor for a circular finned-tube heat exchanger with in-lined arrangement under the dry and wet operation conditions. The foregoing literature review shows that no related work on the circular finned-tube heat exchangers with staggered arrangement under the wet condition has been published. This has motivated the present investigation.

The purpose of this paper is to investigate the pressure drop, heat and mass transfer performances under the dry and wet conditions for two circular finned- tube heat exchangers with staggered arrangement. Experiments were conducted in a steady-state induced draft wind tunnel. In addition, numerical simulations of the laminar, three-dimensional fluid flow and heat transfer over the dry circular finned-tube banks are performed and compared with the experiments.

2. EXPERIMENTAL SET-UP

Two types of finned-tube configurations were tested in the present study and their detailed geometrical parameters are tabulated in Table 1. Experiments were conducted in an induced open wind tunnel as shown in Fig. 1. The ambient temperature and humidity were controlled at 27 ℃ and 70 % by an air-ventilator which can provide a cooling capacity up to 21.2 KW. The air flow was driven by a 3.73 KW centrifugal fan with an inverter to provide various inlet velocities. The air temperatures at the inlet and the exit zones across the test section were measured by two psychometric boxes which are constructed based on ASHRAE 41.1 standard [6]. The pressure of the test coil is detected by a precision differential pressure transducer, readings to 0.1 Pa. The air flow measuring station is an outlet chamber setup with multiple nozzle based on the ASHRAE 41.2[7].

The working medium in the tube side was hot or chilled water. The water temperature was controlled by a thermostat reservoir. In dry condition, the hot water inlet temperature was

controlled at 75℃; in wet condition, the chilled water was controlled at 7.0℃ . Both the water side inlet and outlet temperatures were measured by two pre-calibrated RTDs (pt-100Ω). Their accuracy was within 0.05℃. The water volumetric flow rate was measured by a magnetic volume flow meter with 0.002 L/s resolution. All the data signals were collected and converted by a data acquisition system. Generally, the energy balance between air side and tube side was 3% for dry coils and 7 % for wet coils.

To obtain the average heat transfer coefficients h for the dry coils and the sensible heat transfer coefficient h_s and mass transfer coefficient h_d for the wet coils from the measured experimental data, the ε -NTU (effectiveness-number of transfer unit) method was used for the dry coils and LMHD(log mean enthalpy difference) method was applied for the wet coils. It is noted that the water side resistance was estimated to be less than 10 % of the overall heat resistance. Note that the wall resistance was negligible. Therefore, the dominant thermal resistance was always on the air side. This may resolve any concern about the magnitude and accuracy of the water side that is being subtracted from the overall resistance.

The heat and mass transfer characteristics of the heat exchangers are presented in the following nondimensional groups:

Colburn factor j for dry coil

$$j = \frac{h}{G \cdot c_p} \mathrm{Pr}^{2/3}$$

sensible Colburn factor J_s for wet coil

$$j_s = \frac{h_s}{G \cdot c_p} \mathrm{Pr}^{2/3}$$

mass transfer Colburn factor J_t for wet coil

$$j_t = \frac{h_d}{G} Sc^{2/3}$$

where G is the mass velocity , c_p is the specific heat of the fluid, Pr and Sc are the Prandtl and Schmidt numbers, respectively. The core friction factor f of the heat exchanger is calculated from the pressure drop equation proposed by Kay and London[8]. Uncertainties in the reported experimental values of J, sensible J_s, mass transfer Colburn factor J_t and friction factor f were estimated by the method suggested by Moffat [9]. The uncertainties ranged from 4 % to 7 %.

3. THREE-DIMENSIONAL MATHEMATICAL ANALYSIS

The fluid is considered incompressible with constant properties and the flow is assumed to be laminar, steady, and no viscous dissipation. The dimensionless equations for continuity, momentum and energy may be expressed in tensor form as

$$\frac{\partial U_i}{\partial X_i} = 0$$

$$\frac{\partial}{\partial X_j}\left(U_i U_j\right) = -\frac{\partial P}{\partial X_i} + \frac{1}{\mathrm{Re}_H}\left[\nabla^2 U_i\right]$$

$$\frac{\partial}{\partial X_j}\left(\Theta U_j\right) = \frac{1}{\mathrm{Re}_H \,\mathrm{Pr}}\left[\nabla^2 \Theta\right]$$

In the above equations, the velocity has been nondimensionalized with the uniform inlet velocity w_{in} at the channel inlet, all length coordinates with the fin spacing H, and the pressure with ρw_{in}^2. The dimensionless temperature is defined as $\Theta = (T - T_w)/(T_{in} - T_w)$. The Reynolds number is $\mathrm{Re}_H = w_{in} \cdot H/\nu$,where ν is the kinematic viscosity of the fluid.

Because the governing equations are elliptic in spatial coordinates, the boundary conditions are required for all boundaries of the computation domain. At the upstream boundary, uniform flow with velocity $w_{in}\vec{k}$ and temperature T_{in} are assumed. At the downstream end of the computational domain, located five tube diameters from the last downstream row tube, streamwise gradient (Neumann boundary conditions) for all the

variables are set to zero. At the symmetry planes normal gradients are set to zero. At the solid surfaces, no-slip conditions and constant wall temperature T_w are specified.

The pressure drop is expressed in terms of the dimensionless pressure coefficient, Cp, defined as, $C_p = 2 \cdot (P - P_{in}) / \rho w_{in}^2$, where p_{in} is the pressure at inlet. The local heat transfer coefficient h is defined as $h = q'' / (T_w - T_b)$, where q'' is the local heat flux and T_b is the local bulk mean temperature of the fluid. The local heat transfer coefficient can be expressed in the dimensionless form by the Nusselt number Nu, defined as $Nu = h \cdot H / k$, where k is the thermal conductivity of the fluid.

4. NUMERICAL METHOD

In this study, the body-fitted coordinate system was used to generate a general curvilinear coordinate system numerically by solving Laplace equations with proper control of grid densities. The governing equations are solved numerically using a control volume based finite difference formulation. The SIMPLER algorithm [10] is used to solve iteratively the system of finite-difference equations. The hybrid scheme is employed for the treatment of convection and diffusion terms. A grid system of 15x 19 x 200 grid points is adopted in the computation domain as shown in Fig. 2. Computations were performed on IBM/RS6000 and typical CPU times are 6-7 hours for each case.

4. RESULTS AND DISCUSSIONS

Experimental results of thermal-hydraulic characteristics for the samples A and B under the dry and wet operations are illustrated in Figs. 3-6. Figs. 3 and 4 present the variation of the Colburn j and sensible Colburn j_S factors with the Reynolds number Re for the dry and wet coils, respectively. Also plotted in the figures for the comparison are the correlations developed by Briggs and Young[2] for the dry coils and Idem et al.[4] for the wet coils, which is under the in-lined arrangement. The present dry coil results are in good agreement those of the Briggs and Young [2], while for the wet coils, the correlation developed by Idem et al. [4] is significantly lower than 30-50 % that of the present experimental results. By comparing Figs. 3 and 4, it can be seen that the sensible Colburn factor j_S for the wet coils is 20 % higher than the j factor for the dry coils. The variation of the mass transfer Colburn j_t factor with the Reynolds number is illustrated in Fig. 5. Again, the j_t value for the in-lined arrangement [4] is smaller than 50-100 % that for the staggered arrangement. Fig. 6 shows the dry and wet friction factor f vs. Re for samples A and B. It is noted that the dry friction correlation obtained by Robinson and Briggs [3] is also illustrated in the figure. It is seen that friction factor f for the wet coils is 15 % higher than that for the dry coils. The Idem el al. correlation is significantly lower than that of the present experimental results and therefore is not valid in the present case.

The numerical simulations of the three-dimensional laminar circular finned-tube bank under the dry condition are shown in Figs. 7-10. Figs.7 and 8 present the variations of Nu and Cp, respectively, around the tube surface from the 1st to the 4th row for sample A. The angle θ is measured from front stagnation point of the tube. One can see that variations of the surface pressure profile for each row look similar, and the Cp value decreases in order from the 1st row to the 4th row. It is also seen that the peak value for Nu decreases in order from the 1st row to the 4th row.

The calculated and measure pressure drop and averaged heat transfer coefficient at various inlet front velocity ranging from 2 to 6 m/s are presented in Figs 9 and 10, respectively. The solid lines represent the numerical results for the samples A and B; while the experimental results are denoted by the triangular and rectangular symbols, respectively. It is seen that the numerical results for the pressure drop are in excellent agreement with the experimental data. Although the calculated and experimental results of the average heat transfer coefficients are in the same order of magnitude, the numerical results overestimate the heat transfer coefficient by 200 % . This is due to the fact that the actual boundary conditions for the tube and fin surfaces in the experiment do not occur under the constant wall temperature.

5. CONCLUSIONS

Experimental and numerical predictions of thermal-hydraulic characteristics of circular finned-tube heat exchangers under the dry and wet operation conditions are presented. The sensible Colburn factor j_s and mass transfer Colburn factor j_t for the in-lined arrangement are smaller than 30- 100 % that for the staggered arrangement. The sensible Colburn factor j_S for the wet coils is 20 % higher than that for the dry coils; the friction factor f for the wet coils is 15 % higher than that for the dry coils. Although the three-dimensional numerical results for the pressure drop are in good agreement with the experimental data, they overestimate 200% of the heat transfer coefficient. Therefore, conjugate heat transfer between the fin and tube must be considered for more accurate numerical simulation.

ACKNOWLEDGMENTS

Financial support for this work was provided by the national Science of Taiwan under contract NSC86-2212-E006-089.

REFERENCES

1. Webb, P. L., 1994, *Principles of Enhanced Heat Transfer*, John Wiley and Sons, Inc., New York.

2. Briggs, D. E. and Young, E. H., 1963, Convection Heat Transfer and Pressure Drop of Air Flowing across Triangular Pitch Banks of Finned Tubes, *Chem. Eng. Prog. Symp. Ser.*, Vol. 59, No.41, pp. 1-10.

3. Robinson, K. K. and Briggs, D. E., 1966, Pressure Drop of Air Flowing across Triangular Pitch Banks of Finned Tubes , *Chem. Eng. Prog. Symp. Ser.*, Vol. 62, No.64, pp.177-184.

4. Idem, S. A., Jacobi A. M. and Goldchmidt, V. M., 1990, Heat Transfer Characterization of a Finned-Tube Heat Exchanger (With and Without Condensation) , *Transaction of the ASME* ,Vol. 112 ,pp. 64-70.

5. Idem , S. A. and Goldchmidt, V. M., 1993, Sensible and Latent Heat Transfer to a Baffled Finned-Tube Heat Exchanger , *Heat Transfer Engineering* ,Vol. 14, No.3, pp. 26-35.

6. ASHRAE Standard 41.1, 1986. Standard Method for Temperature Measurement, American Society of Heating , Refrigerating and Air-Conditioning Engineers, Inc., Atlanta.

7. ASHRAE Standard 41.2, 1987, Standard Method for Laboratory Air-Flow Measurement, *American Society of Heating ,Refrigerating and Air-Conditioning Engineers* , Inc., Atlanta.

8. Kay, K. M. and London, A. L., 1984, *Compact Heat Exchangers*, 3rd Ed. McGraw-Hill, New York.

9. Moffat, R. J., 1988, Describing the Uncertainties in Experimental Results, *Exp. thermal Fluid Sci.* Vol. 1, pp. 3-17.

10. Pantaker , S. V., 1988, A Calculation Procedure for Two-Dimensional Elliptic Problem , *Numerical Heat Transfer* ,Vol. 4, pp.409-426.

Table 1 Hear Exchangers Geometrical data

	sample A	sample B
D_i(mm)	14.8	23.2
D_o(mm)	19.1	27
D_e(mm)	43	41
δ(mm)	.4	.5
s(mm)	2.8	2.7
X_T(mm)	63	45
X_L(mm)	54.6	37
tube numbers	24	24
Pass numbers	4	4
HX length(mm)	400	400
HX width(mm)	266	148
HX height(mm)	350	280

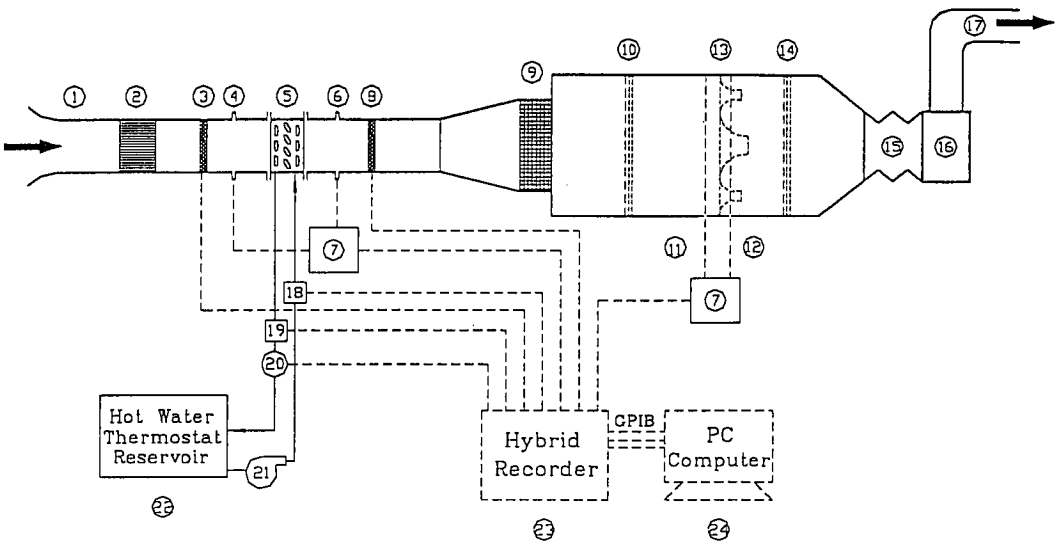

1. inlet
2. air straightener
3. air side inlet temperature measuring station
4. pressure tap(inlet)
5. test section
6. pressure tap(outlet)
7. differential pressure transducer
8. air side outlet temperature measuring station
9. air mixer
10. air straightener
11. nozzle pressure tap(inlet)
12. nozzle pressure tap(outlet)
13. multiple nozzles plate
14. air straightener
15. flexible duct
16. variable exhaust fan system
17. discharge
18. tube side inlet temperature measuring station
19. tube side outlet temperature measuring station
20. volumetric flow meter
21. pump

Fig. 1 Schematic diagram of the experimental setup

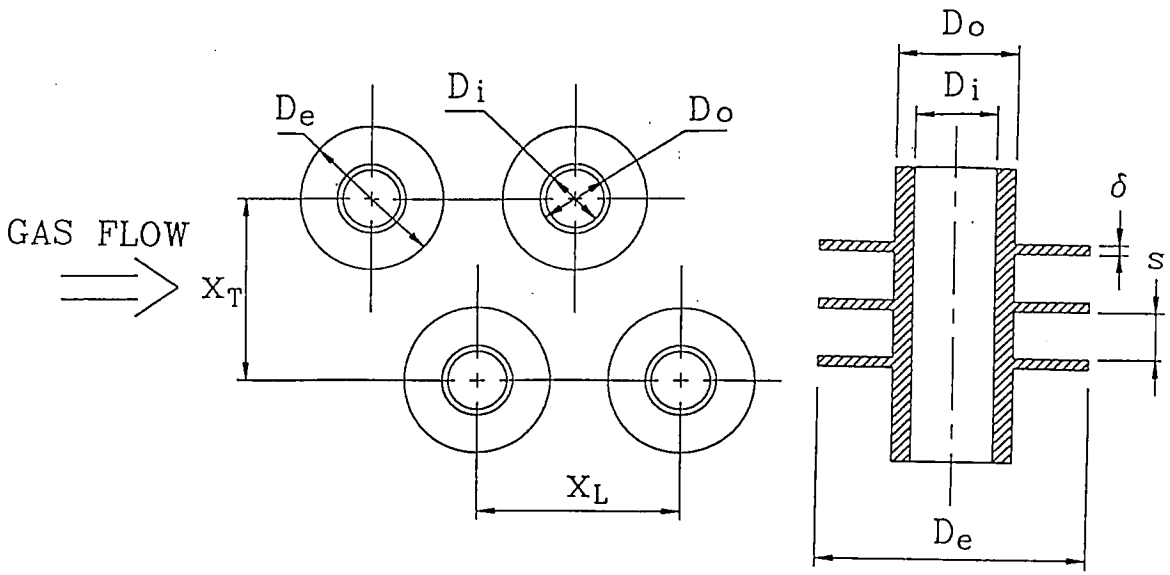

Heat exchanger geometrical data

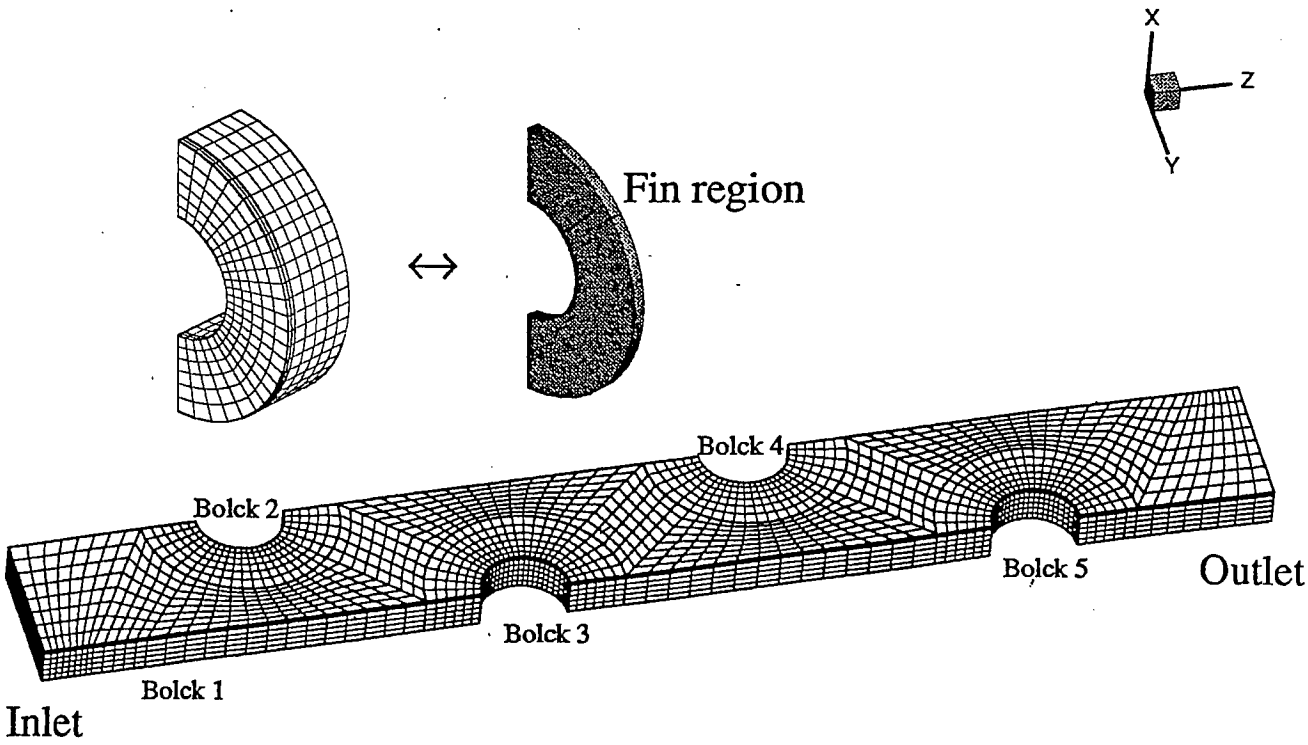

Fig. 2 Computational grid system

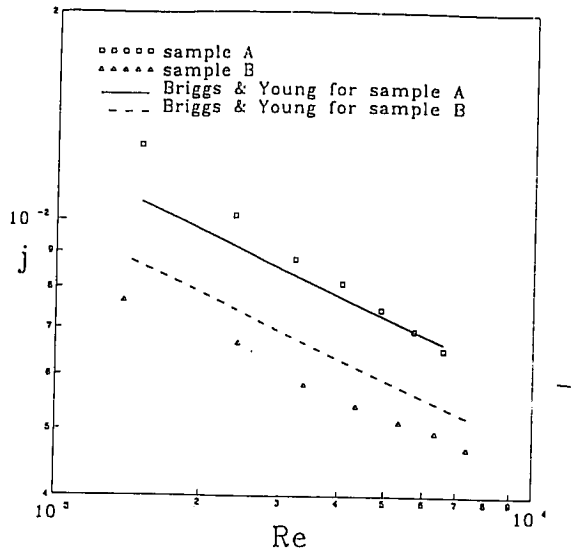

Fig. 3 The variation J factor with Re for the dry coils

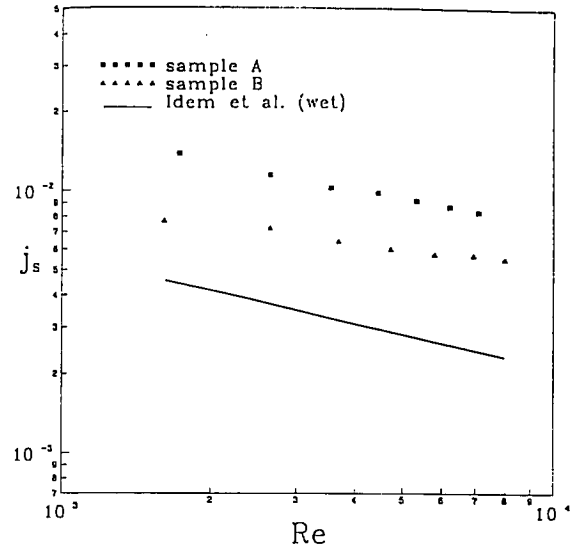

Fig. 4 The variation J_s factor with Re for the wet coils

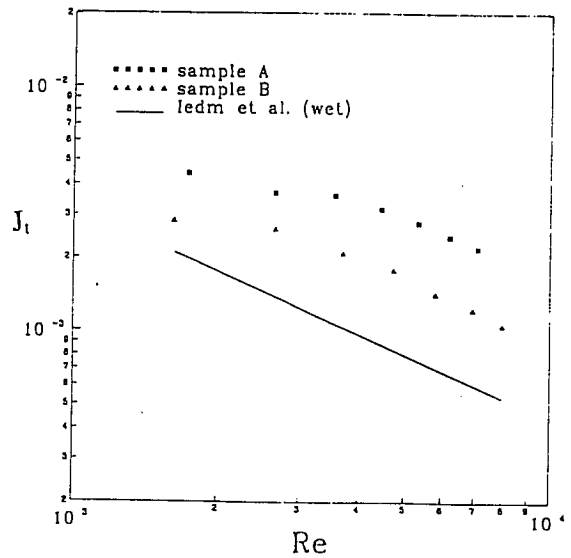

Fig. 5 The variation J_t factor with Re for the dry coils

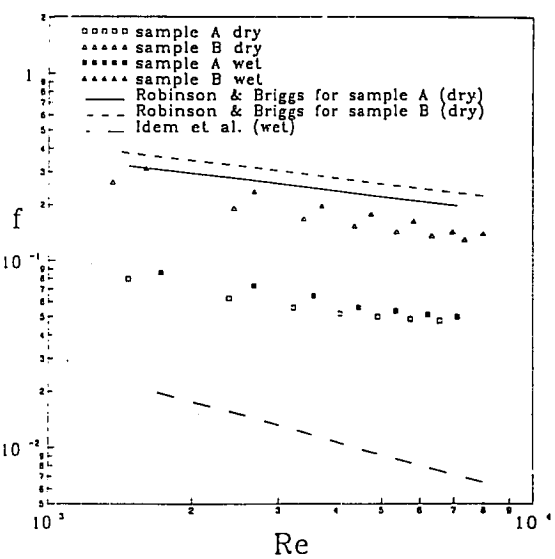

Fig. 6 f vs. Re for the dry and wet coils

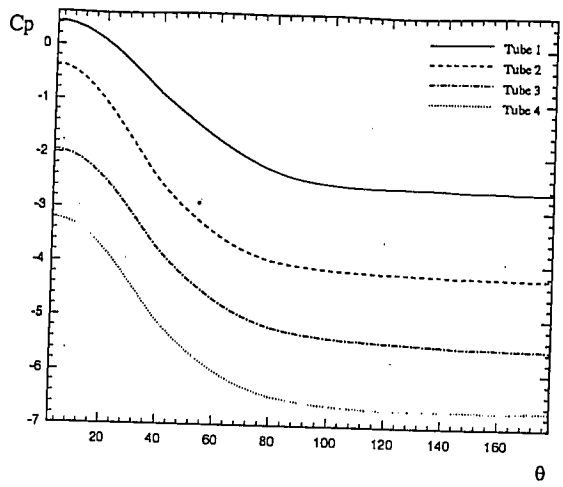

Fig. 7 The variation of Cp around the tube surface for sample A

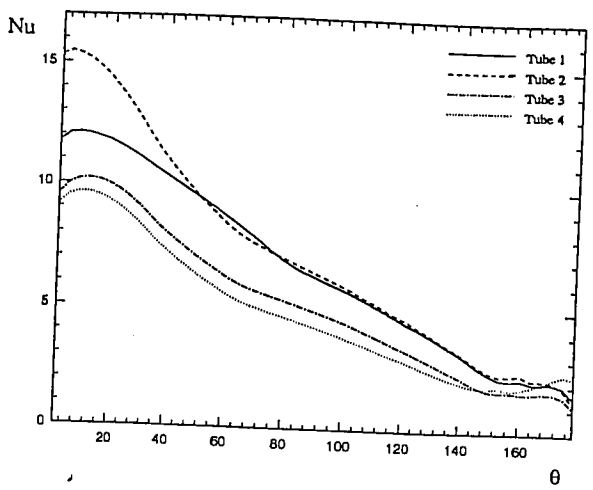

Fig. 8 The variation of Nu around the tube surface for sample A

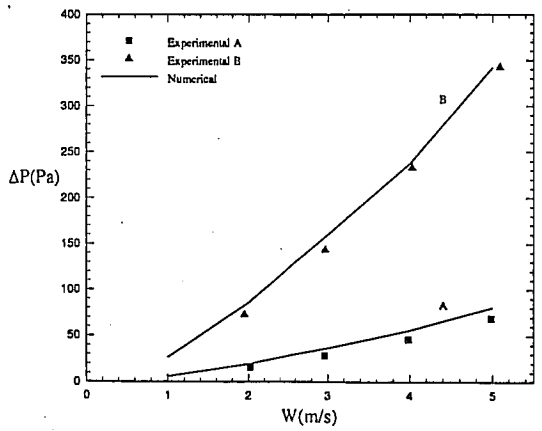

Fig. 9 The calculated and measured ΔP as function of inlet frontal velocity

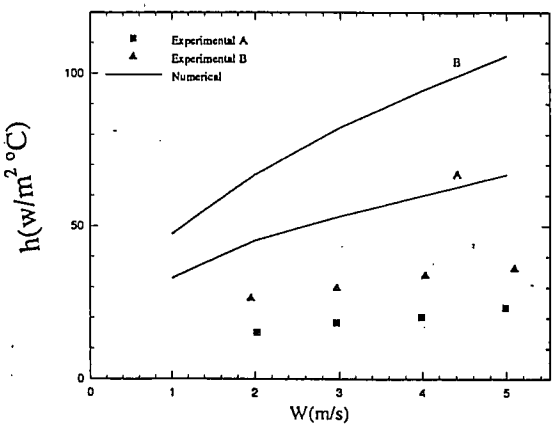

Fig.10 The calculated and measured h as function of inlet frontal velocity